University of South Carolina

Scholar Commons

2011

Optical Cell for Combinatorial *In Situ* Raman Spectroscopic Measurements of Hydrogen Storage Materials at High Pressures and Temperatures

Jason R. Hattrick-Simpers
University of South Carolina - Columbia, simpers@cec.sc.edu

Wilbur S. Hurst

Sesha S. Srinivasan

James E. Maslar

Follow this and additional works at: https://scholarcommons.sc.edu/eche_facpub

Part of the Energy Systems Commons, Engineering Physics Commons, and the Other Chemical Engineering Commons

Publication Info

Jason R. Hattrick-Simpers, Wilbur S. Hurst, Sesha S. Srinivasan, and James E. Maslar

---

Articles you may be interested in

Optical cell for in situ vibrational spectroscopic measurements at high pressures and shear
Rev. Sci. Instrum. **82**, 073905 (2011); 10.1063/1.3606640

Development of a nuclear magnetic resonance system for in situ analysis of hydrogen storage materials under high pressures and temperatures
Rev. Sci. Instrum. **81**, 104101 (2010); 10.1063/1.3484282

A robust volumetric apparatus and method for measuring high pressure hydrogen storage properties of nanostructured materials
Rev. Sci. Instrum. **79**, 063906 (2008); 10.1063/1.2937820

Apparatus for high temperatures and intermediate pressures, for in situ nuclear magnetic resonance of hydrogen storage systems
Rev. Sci. Instrum. **76**, 073906 (2005); 10.1063/1.1979472

In situ high pressure-temperature Raman spectroscopy technique with laser-heated diamond anvil cells
Rev. Sci. Instrum. **75**, 3302 (2004); 10.1063/1.1791811

Optical cell for combinatorial *in situ* Raman spectroscopic measurements of hydrogen storage materials at high pressures and temperatures

Jason R. Hattrick-Simpers,[1] Wilbur S. Hurst,[2] Sesha S. Srinivasan,[3] and James E. Maslar[2]

[1]*Department of Chemical Engineering, University of South Carolina, Columbia, South Carolina 29208, USA*

[2]*Process Measurements Division, National Institute of Standards and Technology, Gaithersburg, Maryland 20899, USA*

[3]*Department of Physics, College of Engineering, Architecture, and Physical Sciences, Tuskegee University, Tuskegee, Alabama 36088, USA*

An optical cell is described for high-throughput backscattering Raman spectroscopic measurements of hydrogen storage materials at pressures up to 10 MPa and temperatures up to 823 K. High throughput is obtained by employing a 60 mm diameter $\times$ 9 mm thick sapphire window, with a corresponding 50 mm diameter unobstructed optical aperture. To reproducibly seal this relatively large window to the cell body at elevated temperatures and pressures, a gold o-ring is employed. The sample holder-to-window distance is adjustable, making this cell design compatible with optical measurement systems incorporating lenses of significantly different focal lengths, e.g., microscope objectives and single element lenses. For combinatorial investigations, up to 19 individual powder samples can be loaded into the optical cell at one time. This cell design is also compatible with thin-film samples. To demonstrate the capabilities of the cell, *in situ* measurements of the $Ca(BH_4)_2$ and nano-$LiBH_4$–$LiNH_2$–MgH_2 hydrogen storage systems at elevated temperatures and pressures are reported. © *2011 American Institute of Physics*. [doi:10.1063/1.3558693]

I. INTRODUCTION

Materials for hydrogen storage in mobile applications need to be capable of storing a large weight percent hydrogen, to have favorable thermodynamics and kinetics, and to be able to be reversibly cycled 1500 times. A single material that meets all of these requirements has yet to be discovered. Therefore, in an attempt to increase the rate at which new materials can be screened some groups have begun to employ combinatorial methodologies for powder and thin-film samples. Zhao *et al.*[1], for instance, developed a parallel ball-milling system that synthesizes powders with multiple compositions simultaneously, and a multichamber Sieverts reactor for hydrogen cycling studies. In the thin-film community, where direct measurements of hydrogen storage on samples with spatially varying composition via volumetric or gravimetric means are not possible, a number of alternative measurement techniques have been proposed. These techniques include measurements of changes in film transparency, changes in stress of a bimorph, changes in normalized emissivity, optical spectroscopy, and x-ray diffraction.[2–6]

With the exception of x-ray diffraction, each of these techniques is an indirect measurement of hydride content that attempts to correlate changes in a secondary property to the hydrogen content of the film. Thus, it is difficult to use these techniques to obtain information about chemical pathways, multiple step transformations, the presence of more than one hydride phase, and the formation of new phases. While x-ray diffraction studies can provide such information, they suffer from the poor scattering efficiencies of the light elements (B, Li, N, and H) used in typical complex hydrides. In contrast, measurement techniques such as Fourier transform infrared (FTIR) spectroscopy and Raman spectroscopy can provide

information about not only the types of chemical bonds present in a sample but also the local bonding environment. FTIR and Raman spectroscopy have been previously shown in single powder samples to provide information regarding the desorption pathway of complex hydride powders.[5,7] However, for FTIR measurements the powders are typically ground with an optically transparent medium. Such intimate contact can cause contamination of the, often nanograined, powder, which could be especially troublesome at higher temperatures.[8] In contrast, for Raman spectroscopy there is no need to place the highly reactive powders in intimate contact with potential contaminates.

Previous *in situ* Raman studies of hydrogen storage materials have largely been concerned with the desorption properties of the material, and have therefore been carried out at pressures near 0.1 MPa.[8–10] Some high pressure *in situ* works have been reported but have involved the use of sapphire or diamond anvil cells to look at high-pressure phase transitions in single fully hydrogenated powders.[11–13] However, the small sampling area for anvil cells precludes the simultaneous measurement of more than one powder.[11,12,14,15]

On the other hand, high-pressure and temperature cells utilizing sapphire windows for Raman spectroscopy have been reported with unobstructed optical apertures on the order of a centimeter in a large number of applications.[16–20] However, there have been few attempts to design such a cell for hydrogen storage materials. A commercially available system was found that would allow for microscope objective based Raman spectroscopic measurements (henceforth referred to as micro-Raman configuration) of combinatorial thin-film samples up to 10 MPa; however, a new optical cell body and heating stage would need to be designed to allow for the measurement of multiple powders. Li *et al.* have

reported a combination FTIR/Raman spectroscopy cell for the *in situ* measurement of powder catalysts.[21] In their report, the Raman spectra are collected from six radially distributed optical windows, each with access to a single powder that has been pressed onto a metal foam substrate. Since thin-film combinatorial samples are generally deposited as a continuously changing composition gradient, the extension of this cell to thin-film combinatorial studies would require the concession of only looking at a few discrete compositions at a time. Also, the cell would have to be redesigned to permit the use of multiple extended focus microscope objectives. It would be preferable for multiscale combinatorial studies if the optical cell would allow for facile switching from a thin-film combinatorial measurement configuration to one that allows measurements on powder arrays.

Here we report on a high-pressure and temperature optical cell designed to allow studies of hydrogen storage combinatorial thin films or multiple powders through back-scattered Raman spectroscopic measurements. The cell incorporates a 60 mm diameter × 9 mm thickness sapphire window, which corresponds to a 50 mm diameter unobstructed optical aperture and can withstand hydrogen pressures of up to 10 MPa and temperatures up to 823 K. The sample stage height can be easily adjusted so that measurements can be made either in an achromatic or singlet lens-based optical configuration (henceforth referred to as a macro-Raman configuration) or in a micro-Raman configuration. The powders are packed into Mo cups, which are then mounted onto a sample heating stage that promotes temperature uniformity in the powders. To illustrate the capabilities of the chamber *in situ* measurements of the $Ca(BH_4)_2$ and the nano-$LiBH_4$–$LiNH_2$–MgH_2 hydrogen storage systems at elevated temperatures and pressures are demonstrated.

II. CELL DESIGN

A cross sectional view of the assembled optical cell is shown in Fig. 1. The main cell body is a standard 114.3 mm (4.5 inch) Conflat[22] (CF) nipple. The body material is made from 316LN stainless steel, which was chosen for its superior resistance to hydrogen embrittlement. The window assembly (described in the following section) is shown mounted at the top of the optical cell, while a heating stage/electrical feedthrough assembly is shown mounted to the bottom. Both assemblies were formed using machined 316LN steel 114.3 mm (4.5 inch) CF flanges, and were sealed at the flange with standard Cu gaskets. Cu tends to be embrittled by hydrogen over relatively long periods of time; therefore to prevent hydrogen embrittlement of the gaskets resulting in failure of the seal, both gaskets are changed after each experiment.

The heating stage/electrical feedthrough assembly has radially distributed tapped holes to accommodate four commercially available high-pressure electrical feedthroughs, which are rated for pressures up to 55 MPa and 1143 K. A base, with a centrally located tapped hole to support a threaded brass rod, is mounted on the inside of the flange. The sample heating stage is attached to the top of the threaded rod. The threaded rod allows for the relative position of the heating stage to the sapphire window to be adjusted from 1 to 20 mm. This
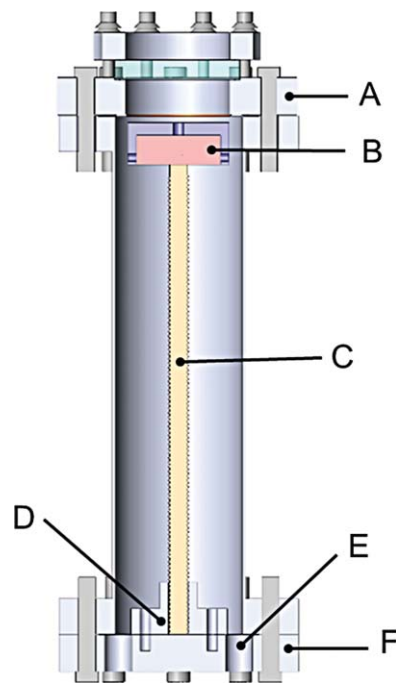

FIG. 1. (Color online) Cross sectional schematic view of *in situ* optical cell. A indicates the window assembly, B the assembled heating stage, C the threaded rod, D the mounted base, E the placement of the electrical feedthroughs, and F is the heating stage/electrical feedthrough assembly.

permits measurements taken in either a macro- or a micro-Raman configuration without having to use a different cell.

The substrate heater is a 40.64 mm diameter BN heater capable of reaching 1073 K in reactive environments. The use of BN as the heating stage material prevents chemical attack by the hydrogen gas during high-temperature high-pressure measurements. The temperature uniformity of the heater is rated to be <2% across the entire hot zone. The heater temperature is monitored by a single type K thermocouple, which is mounted so that it is in direct contact with the back plate of the heater. The temperature is controlled to within ±1 K by an external power supply. No additional sealing is required for the substrate heater, since the entire substrate heater is contained within the pressure cell, and all the electrical connections are obtained via the high-pressure electrical feedthroughs.

A single 6.35 mm (1/4 inch) stainless steel compression fitting (not shown) was welded to the cell body as a gas inlet/vacuum line. A high-pressure three-way valve with 6.35 mm (1/4 inch) compression fittings was then mounted onto the fitting as a gas inlet/vacuum line. The assembled optical cell is small enough to be able to fit through a 41 cm diameter × 57 cm deep glove box exchange chamber, allowing for sample mounting and transport without exposing the samples to ambient conditions.

During experiments on powders the samples are first packed into 6.5 mm (1/4in.-20) Mo set screws that serve as sample cups. Mo was chosen to hold the powders because it has limited reactivity with typical hydrogen storage materials such as Li and Mg, a relatively high thermal conductivity (139 W m^{-1} K^{-1}), and a high melting temperature of 2896 K. The Mo set screws are mounted into one of two faceplates, which are fixed to the top of the substrate heater. The first
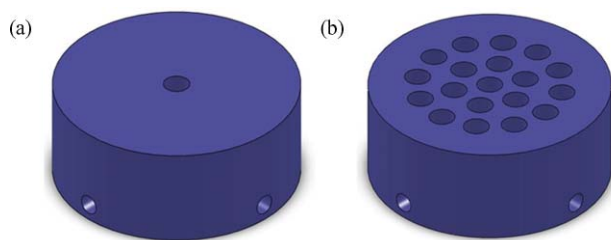
FIG. 2. (Color online) Isometric views of Al single powder sample holder (a) and Mo high-throughput sample holder (b).

faceplate is fabricated from Al [shown in Fig. 2(a)], and is used for single powder measurements up to 773 K (about 160 K below the melting temperature of Al). Al was chosen for its excellent thermal conductivity and ease of machining. The second faceplate is fabricated from Mo [Fig. 2(b)], chosen for the same reasons described earlier for the set screws, and has 19 radially distributed tapped through-holes for sequential measurements of multiple powders. Threaded through-holes are used so that during measurements the bottom of the set screws are in direct contact with the heater face, improving the temperature uniformity. Thin-film combinatorial samples can be mounted using clips onto a thin Al plate, which screws into the Al faceplate.

III. WINDOW DESIGN AND SEALING

The window assembly (Fig. 3) is composed of a 114.3 mm (4.5 inch) CF flange with a centered 50 mm diameter counter bore. The outside of the flange was counter bored to have a 3 mm deep × 60 mm diameter recess for window seating. The window is a 60 mm diameter × 9 mm thickness sapphire window oriented with its c-axis parallel to the window face. Sapphire was chosen as the window material due to its high elastic modulus (340 GPa), its excellent transparency, its resistance to chemical attack, and its high apparent elastic limit (>275 MPa).

For materials with nonlinear stress–strain relationships, it is common practice to approximate the elastic limit as an apparent elastic limit, defined as the stress at which the rate

of strain is 50% greater than the zero stress.[23] The factor of safety for a window is then defined as the ratio of the apparent elastic limit of the window material to the highest stress it will experience in practical operation, and it is recommended that this value be between 3 and 4 for a pressure vessel.[24] The apparent elastic limit of sapphire is commonly reported in literature as being 448 MPa.[16,25]

The factor of safety was calculated using the formula from Hughes *et al.*:[26]

$$S = \frac{T^2 M_r}{1.1 P D^2},$$

where D is the unsupported diameter of the window, S is the safety factor, P is the differential pressure, T is the thickness, and M_r is the apparent elastic limit. The 1.1 is an additional multiple that is incorporated to minimize the likelihood of window failure. Here the factor of safety is found to be 3.65, well within the acceptable range for pressure cells.

Sealing of the window was accomplished using a metal-to-window seal similar to the report by Bowers *et al.*[17] Specifically, two 0.25 mm diameter gold wires were cut to length, welded using a hydrogen/oxygen torch, and then annealed at 1223 K in air for 1 h to form two o-rings. One o-ring was placed between the CF flange and the window to form the pressure seal. The second o-ring was inserted between the window and the top faceplate to prevent direct contact between the faceplate and the window to help minimize the chance of window cracking due to point contact.

Eight bolts in the faceplate were torqued to 5 Nm to form a gas tight seal, as confirmed by performing a helium leak check. Multiple spring washers were employed on each bolt to maintain pressure on the window, and to compensate for the difference in the thermal expansion coefficients of the window and the stainless steel flange. The spring washers were chosen to exert 3.5 kN of force at half their travel, and to ensure that their total travel was greater than the difference in the thermal expansion coefficients of the sapphire and the stainless steel.

These seals were found to be reliable up to 10 MPa without failure of the o-rings. Repeated high temperature cycling of the cell over a period of 1 year was found to cause the o-rings to adhere to the stainless steel, resulting in a degraded seal. Once the o-ring had degraded such that it could not form an adequate seal, determined by a He leak check, the window assembly was taken apart, the flange was polished to remove the residual gold, and the system was reused.

There are three primary advantages to the window design used in this study. The first is that the large window size and simple geometry allow the cell to be used for a number of other optical measurement techniques. The optical cell reported here has also been utilized for normalized IR emissivity measurements and FTIR spectroscopic measurements on thin-film samples. The same cell could also be used for a variety of other measurement techniques including reflectivity/transparency measurements or optical measurements of cantilevers during gas loading/temperature actuation.

The second advantage is that the windows are easily removed and replaced between measurements. Since there is no physical constraint regarding the thickness of the window used with the cell, and only the combination of the window
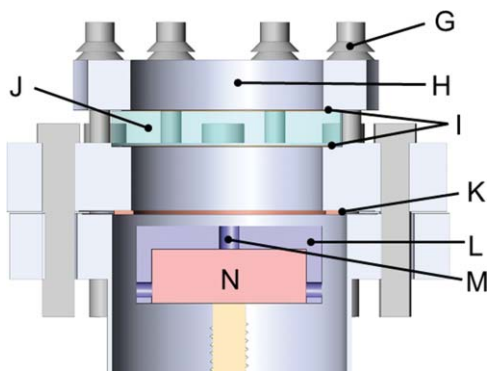

FIG. 3. (Color online) Side view of the optical cell showing the sample stage and window region. G indicates the spring washers, H the top faceplate, I the two Au o-rings, J the sapphire window, K the copper gasket, L the heater's faceplate (with one set screw hole), M the Mo set screw, and N is the sample heater.

thickness, apparent elastic limit, and diameter determines the operable pressure range of the cell, the window material used is somewhat arbitrary. For instance, 10 mm thick ZnSe windows, which permit transmission of radiation from 5000 to 450 cm^{-1}, were employed to observe infrared absorptions near 1000 cm^{-1} in MgH_2 thin films during *in situ* hydrogenation at 0.5 MPa.

The third advantage of this cell is the ability to switch between micro- and macro-Raman configurations without making substantial changes to the optical cell. The high power density that would result from micro-Raman measurements on a powder sample can result in powder heating, thereby complicating the interpretation of thermodynamic measurements. Therefore, the use of a macro-Raman configuration is preferred when investigating powder samples. On the other hand, Raman spectroscopic measurements on thin films are often done employing a micro-Raman configuration, where the collection efficiency of the Raman scattered light is maximized.

IV. *IN SITU* RAMAN SPECTROSCOPIC MEASUREMENTS

To demonstrate the capabilities of the optical cell, Raman spectroscopic measurements of $Ca(BH_4)_2$ and nano-$LiBH_4$–$LiNH_2$–MgH_2 powders were conducted. The preparation of both powders has been discussed elsewhere.[27,28] The powders were handled and loaded into the optical cell inside an Ar filled glove box with a water concentration less than 1.11×10^{-7} mol H_2O/mol Ar (0.05×10^{-6}). Generally, 4–8 mg of powder was weighed and packed into a Mo set screw. The set screw was then mounted into the heating plate, the cell was sealed, and backfilled with ultra high purity (UHP purity >99.9995%) Ar. Prior to removal from the glove box, the cell was pressure tested at a pressure of 0.49 MPa using UHP Ar for 1 h. The total time required for powder loading and pressure testing is less than 2 h. This represents a significant reduction in the time required to measure individual powders.

Many hydrogen storage materials, such as $LiBH_4$, $Li_4BN_3H_{10}$, and $NaAlH_4$, melt prior to releasing hydrogen, which can cause the material to violently bubble and accumulate on the optical windows of the cell. This produces spurious changes to the Raman spectra. It was found that measurements performed under static positive pressures of Ar yielded Raman spectra free of this artifact. Ar was chosen to minimize the hydrogen background during measurements, providing a kinetic measurement of hydrogen desorption without significantly altering the thermodynamics of the powders. Therefore, during hydrogen desorption measurements for both powders, the chamber was filled to a static pressure with 0.49 MPa (5 bar) of UHP Ar.

Raman spectroscopic measurements were performed in a backscattering geometry using 514.5 nm radiation from an argon ion laser (Fig. 4). Approximately 50 mW of laser radiation was focused onto the powder with a 300 mm focal length spherical lens. Scattered radiation was collected and collimated with an *f*/4 achromatic lens located at infinite conjugate ratio. A detailed description of the Raman spectroscopic measurement system can be found in Ref. 5. All spectra were
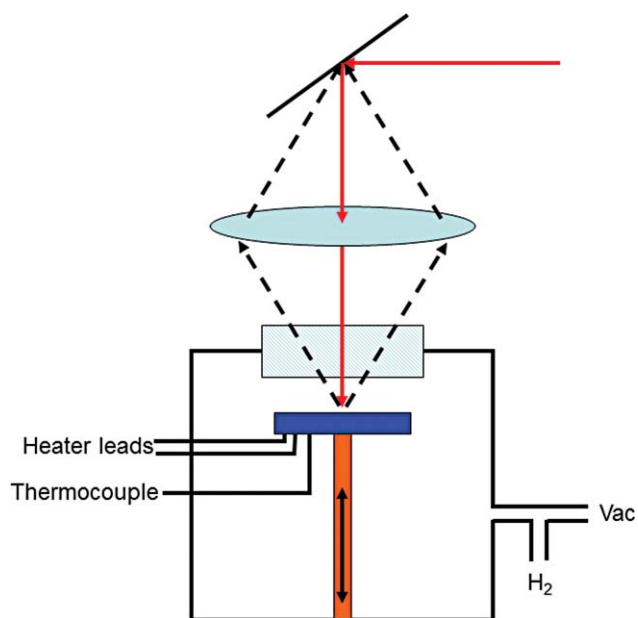
FIG. 4. (Color online) Schematic representation of the experimental geometry.

obtained in integration times of 6 s or less. The Raman spectral positions were determined by fitting the respective spectral peaks at each temperature with Lorentzian line shapes.

To demonstrate the temperature range under which this cell can be operated, the Raman spectra of $Ca(BH_4)_2$ in the spectral region of the B–H stretching modes were recorded as a function of temperature from 298 to 748 K at a ramp rate of 20 K/min. In Fig. 5 the spectra recorded at temperatures from 298 to 698 K are shown (the spectrum recorded at 748 K was nominally identical to the spectrum obtained at 698 K and, therefore, were omitted for clarity). X-ray diffraction measurements (not shown) indicate that the $Ca(BH_4)_2$ powder investigated here is composed of a nearly 1:1 mixture
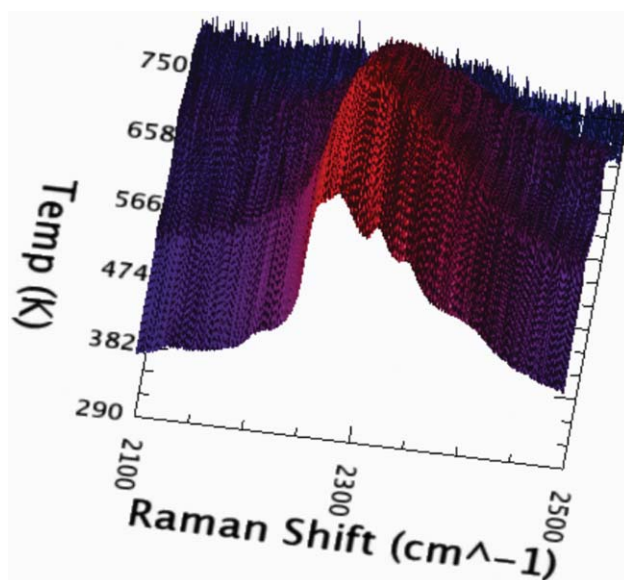
FIG. 5. (Color online) *In situ* Raman spectra of the $Ca(BH_4)_2$ as a function of temperature.

of α- and β-Ca(BH$_4$)$_2$ at room temperature. Therefore, the broad feature in the 298 K spectrum is attributed to a combination of four relatively intense first order α-Ca(BH$_4$)$_2$ B–H stretching modes observed at $\approx$2274, $\approx$2327, $\approx$2352, and $\approx$2415 cm^{-1} (Refs. 8 and 29) and one relatively intense first order β-Ca(BH$_4$)$_2$ B–H stretching mode observed at $\approx$2290 cm^{-1},[8] all superimposed on a number of weaker second order B–H bending combination and/or overtone modes in the $\approx$2100 to $\approx$2600 cm^{-1} range.[29]

In the spectrum obtained at 353 K, the α-Ca(BH$_4$)$_2$ modes are observed at approximately the same wavenumbers as in the 298 K spectrum but at lower intensities relative to other features in the spectrum. In addition, the maximum scattering intensity in the 353 K spectrum is observed at $\approx$2286 cm^{-1} rather than at $\approx$2290 cm^{-1} as in the 298 K spectrum. Assuming a similar dependence of scattering intensity on temperature for all phases this decrease in relative intensity indicates that the α-Ca(BH$_4$)$_2$ phase is relatively less crystalline and/or present in lower relative amounts compared to the other phases in the Raman scattering volume at 353 K compared to 298 K. The decrease in relative intensity of the α-Ca(BH$_4$)$_2$-related modes would be consistent with a phase transformation of α-Ca(BH$_4$)$_2$ (to a phase with a different Raman spectrum). The increase in relative scattering intensity at $\approx$2286 cm^{-1} could also be related to the conversion of α-Ca(BH$_4$)$_2$ to another phase. It is possible that these differences in the Raman spectra obtained at these two temperatures are due to the phase transformation of α-Ca(BH$_4$)$_2$ to α'-Ca(BH$_4$)$_2$ which reportedly occurs when α-Ca(BH$_4$)$_2$ is heated, and continues up to $\approx$495 K.[30] No α-Ca(BH$_4$)$_2$-related features are observed in spectra recorded at 433 K and above. This is attributed to the transformation of the α-Ca(BH$_4$)$_2$ phase to the β-Ca(BH$_4$)$_2$ phase which occurs in the $\approx$440 to $\approx$573 K range,[30,31] and possibly to the continued transformation to the α'-Ca(BH$_4$)$_2$ phase. The spectra obtained at 433–648 K all show a broad, asymmetric feature with a shoulder on the high wavenumber side. As temperature increases, the apparent maximum scattering intensity of this feature shifts from $\approx$2295 cm^{-1} in the 433 K spectrum to $\approx$2315 cm^{-1} in the 648 K spectrum. Since all low temperature phases should transform to β-Ca(BH$_4$)$_2$ by $\approx$573 K,[30,31] the $\approx$2315 cm^{-1} peak in the 648 K spectrum is attributed solely to β-Ca(BH$_4$)$_2$. The similarity of this feature in the 648 K spectrum to those in the 433–598 K spectra suggests that at least some of this scattering is due to the β-Ca(BH$_4$)$_2$ phase. The most intense feature in the β-Ca(BH$_4$)$_2$ spectrum at room temperature has been reported in the $\approx$2290 to $\approx$2300 cm^{-1} range.[8] Assuming the attribution of this mode to the β-Ca(BH$_4$)$_2$ phase in all of these spectra is correct and that no new phases are being formed, the reason for the increase in Raman shift with increasing temperature is unknown. Temperature-induced anharmonic effects tend to result in a decrease in Raman shift.[32] Perhaps this increase in Raman shift is related to an annealing effect as the low temperature α-Ca(BH$_4$)$_2$/β-Ca(BH$_4$)$_2$ mixture is heated to form relatively pure β-Ca(BH$_4$)$_2$ at high temperature. Upon heating, presumably the β-Ca(BH$_4$)$_2$ phase crystalline domain size increases and/or the defect density decreases. No features are observed in the spectra obtained at 698 and
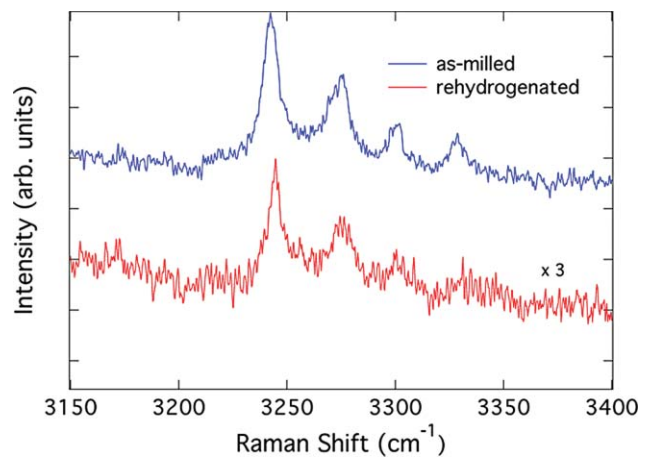

FIG. 6. (Color online) Raman profile of an as-milled powder and a sample that has been desorbed until only the Li$_2$Mg(NH)$_2$ Raman modes are visible and then rehydrogenated at 423 K and 8 MPa. Both Li$_4$BN$_3$H$_{10}$ and Mg(NH$_2$)$_2$ have reformed, and the ratio of their Raman mode intensities is comparable to their as-milled state. Reprinted with permission from J. R. Hattrick-Simpers, J. E. Maslar, M. U. Niemann, C. Chiu, S. S. Srinivasan, E. K. Stefanakos, and L. A. Bendersky, Int. J. Hydrogen Energy **35**, 6323 (2010). Copyright 2010, Elsevier.

748 K. This is attributed to the decomposition of Ca(BH$_4$)$_2$ which is expected in the $\approx$620 and $\approx$770 K range.[30,31]

To illustrate high-pressure rehydrogenation using the optical cell, the reversible nano-LiBH$_4$–LiNH$_2$–MgH$_2$ powder system was cycled *in situ*. The Raman spectra in the region of the N–H stretches for the as-milled powders are shown in Fig. 6. The powder Raman spectrum exhibits four N–H stretching features at 3243, 3274, 3300, and 3329 cm^{-1}. The two peaks at 3243 and 3300 cm^{-1} are attributed to the Li$_4$BN$_3$H$_{10}$ phase.[7] The two peaks at 3274 and 3329 cm^{-1} are attributed to the Mg(NH$_2$)$_2$ phase, the N–H stretching modes of which have been observed at 3277 and 3326 cm^{-1} in an infrared spectrum of Mg(NH$_2$)$_2$.[33] A more detailed study of the as-received powders and their desorption pathway can be found elsewhere.[5]

The powders were first dehydrogenated in 0.49 MPa of UHP Ar at 423 K for 1 h, by which time all of the Raman modes associated with Li$_4$BN$_3$H$_{10}$ and Mg(NH$_2$)$_2$ were no longer observed. Upon completion of the dehydrogenation the chamber was attached to a Sieverts apparatus and pumped down to 5 $\times$ 10^{-5} Pa, flushed with 0.5 MPa of Ar, and then pumped out again. The powders were then rehydrogenated *in situ* under 8 MPa of UHP H$_2$ (purity >99.999%) at 423 K for 1 h. During the hydrogen exposure the Raman peaks for Li$_4$BN$_3$H$_{10}$ and Mg(NH$_2$)$_2$ reappear (Fig. 5), indicating the reversal of the decomposition of those two phases.

V. CONCLUSION

A high-pressure, high-temperature optical cell for performing high-throughput Raman spectroscopic measurements on hydrogen storage thin film and powder samples has been developed. A 50 mm diameter optical aperture is obtained using a 60 mm sapphire window. The cell can be pressurized up to 10 MPa at temperatures as high as 823 K. Window sealing is accomplished using gold o-rings at the metal-to-

window interface. The adjustable sample stage-to-window distance enables facile switching from measurements of thin-film combinatorial samples using micro-Raman to measurements of powder samples using macro-Raman. Raman spectroscopic measurements on $Ca(BH_4)_2$ and nano-$LiBH_4$–$LiNH_2$–MgH_2 were used to demonstrate the capabilities of the cell at high temperatures and high pressures.

ACKNOWLEDGMENTS

[1] J. C. Zhao, *Department of Energy Annual Merit Review and Peer Evaluation* (2006) available at: http://www.hydrogen.energy.gov/annual_review06_storage.html

[2] G. Garcia, R. Domenech-Ferrer, F. Pi, J. Santiso, and J. Rodriguez-Viejo, J. Comb. Chem. **9**, 230 (2007).

[3] R. Gremaud, C. Broedersz, D. Borsa, A. Borgschulte, P. Mauron, H. Schreuders, J. Rector, B. Dam, and R. Griessen, Adv. Mater. **19**, 2813 (2007).

[4] H. Oguchi, J. R. Hattrick-Simpers, and I. Takeuchi, Rev. Sci. Instrum. **80**, 073707 (2009).

[5] J. R. Hattrick-Simpers, J. E. Maslar, M. U. Niemann, C. Chiu, S. S. Srinivasan, E. K. Stefanakos, and L. A. Bendersky, Int. J. Hydrogen Energy **35**, 6323 (2010).

[6] A. Ludwig, J. Cao, A. Savan, and M. Ehmann, J. Alloys Compd. **446**–**447**, 516 (2007).

[7] J. Yang, A. Sudik, D. Siegel, D. Halliday, A. Drews, R. Carter, C. Wolverton, G. Lewis, J. Sachtler, J. Low, S. Faheem, D. Lesch, and V. Ozolins, Angew. Chem. Int. Ed. **47**, 882 (2008).

[8] M. Fichtner, K. Chlopek, M. Longhini, and H. Hagemann, J. Phys. Chem. C **112**, 11575 (2008).

[9] S. Gomes, H. Hagemann, and K. Yvon, J. Alloys Compd. **346**, 206 (2002).

[10] S. Orimo, Y. Nakamori, and A. Zuttel, Mater. Sci. Eng. B **108**, 51 (2004).

[11] R. S. Kumar, E. Kim, O. Tschauner, and A. L. Cornelius, Phys. Rev. B **75**, 174110 (2007).

[12] A. V. Talyzin, O. Andersson, and B. Sundqvist, J. Solid State Chem. **180**, 510 (2007).

[13] C. Wong and P. J. Miller, J. Energ. Mater. **23**, 169 (2005).

[14] L. George, V. Drozd, H. Couvy, J. Chen, and S. K. Saxena, J. Chem. Phys. **131**, 074505 (2009).

[15] R. J. Karpowicz and T. B. Brill, J. Phys. Chem. **84**, 348 (1984).

[16] R. S. Addleman, J. W. Hills, and C. M. Wai, Rev. Sci. Instrum. **69**, 3127 (1998).

[17] W. J. Bowers, Jr., V. E. Bean, and W. S. Hurst, Rev. Sci. Instrum. **66**, 1128 (1995).

[18] J. Lin, M. Santoro, V. V. Struzhkin, and H. Mao, Rev. Sci. Instrum. **78**, 3302 (2004).

[19] J. E. Maslar, W. S. Hurst, and W. J. Bowers, J. Electrochem. Soc. **147**, 2532 (2000).

[20] S. F. Rice, R. R. Steeper, C. A. LaJeunesse, R. G. Hanush, J. D. Aiken, Design strategies for optically-accessible, high-temperature, high-pressure reactor cells, Sandia National Laboratories Report No. SAND99-8260 (Sandia National Laboratories, Albuquerque, NM, 2000).

[21] G. Li, D. Hu, G. Xia, J. M. White, and C. Zhang, Rev. Sci. Instrum. **79**, 074101 (2008).

[22] Certain commercial equipment, instruments, or materials are identified in this document. Such identification does not imply recommendation or endorsement by the National Institute of Standards and Technology, nor does it imply that the products identified are necessarily the best available for the purpose.

[23] Glossary of Materials Testing Terms Instron, 2010. Available at: http://www.instron.us/wa/resourcecenter/glossaryterm.aspx?ID = 50.

[24] R. W. Nichols, *Pressure Vessel Codes and Standards* (Elsevier Applied Science, New York, 1987).

[25] C. Carboni, W. K. Robinson, and H. F. Gleeson, Meas. Sci. Technol. 1236 (1993).

[26] M. E. Hughes and J. L. Fasching, J. Chromatogr. Sci. **23**, 535 (1985).

[27] Y. Filinchuk, E. Rönnebro, and D. Chandra, Acta Mater. **57**, 732 (2009).

[28] M. Niemann, S. Srinivasan, A. Kumar, E. Stefanakos, D. Goswami, and K. McGrath, Int. J. Hydrogen Energy **34**, 8086 (2009).

[29] A. Liu, S. T. Xie, S. Dabiran-Zohoory, and Y. Song, J. Phys. Chem. C **114**, 11635 (2010).

[30] Y. Filinchuk, E. Ronnebro, and D. Chandra, Acta Mater. **57**, 732 (2009).

[31] J. H. Kim, S. A. Jin, J. H. Shim, and Y. W. Cho, J. Alloys Compd. **461**, L20 (2008).

[32] M. Balkanski, R. F. Wallis, and E. Haro, Phys. Rev. B **28**, 1928 (1983).

[33] G. Linde and R. Juza, Z. Anorg. Allg. Chem. **409**, 199 (1974).